A Comparative Study on the Electrochemical Corrosion Behavior of Microcrystalline and Nanocrystalline Aluminum in Natural Seawater

El-Sayed M. Sherif[1,2,], Hany Rizk Ammar[3], Khalil Abdelrazek Khalil[4,5]*

[1]Center of Excellence for Research in Engineering Materials (CEREM), Advanced Manufacturing Institute, King Saud University, P. O. Box 800, Al-Riyadh 11421, Saudi Arabia
[2]Electrochemistry and Corrosion Laboratory, Department of Physical Chemistry, National Research Centre (NRC), Dokki, 12622 Cairo, Egypt
[3]Metallurgical and Materials Engineering Department, Faculty of Petroleum and Mining Engineering, Suez University, Suez, Egypt
[4]Mechanical Engineering Department, College of Engineering, King Saud University, P.O. Box 800, Al-Riyadh 11421, Saudi Arabia
[5]Mechanical Design and Materials Department, Faculty of Energy Engineering, Aswan University, Aswan, Egypt
[*]E-mail: esherif@ksu.edu.sa; emsherif@gmail.com

In this study, we compared the electrochemical corrosion behavior of a newly fabricated nanocrystalline pure aluminum to another microcrystalline aluminum using various electrochemical techniques in natural Arabian Gulf seawater. The nanocrystalline Al was fabricated using mechanical alloying technique. Cyclic potentiodynamic polarization showed that microcrystalline has lower corrosion current and corrosion rate with higher polarization resistance compared to the nanocrystalline Al. The change of current with time at -550 mV vs. Ag/AgCl revealed that the nanocrystalline Al had higher absolute currents. The scanning electron microscopy images showed that nanocrystalline Al surface was more corroding under the aggressiveness action of the seawater and the applied anodic potential value. This was also confirmed by the electrochemical impedance spectroscopy data, which indicated that the nanocrystalline Al shows lower polarization and solution resistances when compared to the microcrystalline Al. All results were in good agreement showing clearly that the nanocrystalline Al has less corrosion resistance and high corrosion rate in the Arabian Gulf seawater due to the presence of many active centers on its surface.

1. INTRODUCTION

Aluminum and its alloys have many characteristic properties like their low density, excellent workability, high thermal and electrical conductivities, and good corrosion resistance [1-4]. Therefore, Al and Al base alloys have been widely used as a material in the fields of transport, building, electrical engineering, household appliances, containers, aircraft and aerospace, etc. The use of these alloys in industry is limited by their relatively low yield stress and corrosion problems when exposed to a harsh environment such as Arabian Gulf seawater or chloride solutions [5-7]. It has been reported [5-11] that Al and its alloys develop a compact, adherent, and continuous oxide film on their surfaces upon exposure to the atmosphere or aqueous solutions. The formation of aluminum oxide film does not have the ability to protect the surface in corrosive media such as natural seawater and solutions containing high chloride concentrations where, aluminum suffers both uniform and pitting corrosion [9-12]. This occurs because of the breakdown of the oxide film as a result of the corrosiveness attack of chloride ions that present in those media.

In order to enhance the corrosion resistance of metals, many ways have been developed, e.g. adding passive alloying elements, applying corrosion inhibitors, applying protective coatings, refining the grain size of the metals from the microscale to nanoscale structure, etc. The principles of nanotechnology are being used to introduce nanocrystalline metals and alloys with excellent mechanical properties and different corrosion resistance. The use of nanotechnology in changing the corrosion resistance of metals and alloys through changing the microstructure of these materials to be less than 100 nm has been reported by several investigators [13-19]. Nanocrystalline materials are characterized by their small grain sizes (<100 nm) and high volume fraction of grain boundaries, which often give rise to unique physical, chemical and mechanical properties compared with those of their cast counterparts [16,17].

Our current work aims to fabricate a new nanocrystalline pure aluminum and to compare its electrochemical corrosion behavior with a microcrystalline pure aluminum in Arabian Gulf seawater. Aluminum matrix composites can be fabricated in the solid state through powder metallurgy (P/M) technique. The P/M method is used due to its great versatility and low cost of production. The process of P/M fabrication consists in mixing the hardening particles with the metallic powders followed by consolidation and sintering [20-22]. The electrochemical corrosion behavior for the tested materials was performed using cyclic potentiodynamic polarization, chronoamperometric current-time and electrochemical impedance spectroscopy measurements. The study was complemented using scanning electron microscopy and X-ray energy dispersive investigations.

2. EXPERIMENTAL DETAILS

2.1. Chemicals, materials, and fabrication of nanocrystalline aluminum

An aluminum rod (Al, 99.99% in purity, 6.5 mm in diameter) was purchased for Aldrich, UK. The naturally aerated stagnant seawater was Arabian Gulf Water and was obtained from the eastern region of the Arabian Gulf (Jubail, Dammam, Kingdom of Saudi Arabia). The nanocrystalline

aluminum rod (spec pure and 6.5 mm in diameter) was fabricated from as-received aluminum powder (size ≈ 100 μm) using the mechanical alloying technique. Where, the ball milling process was carried out under inert atmosphere of high purity Argon ,99.999%; ball-to-powder weight ratio (BPR) of 90:1; speed of rotation of 300 rpm, and milling time of 6 h. An amount of 3 wt% of stearic acid (as a process control agent) was added to the powder in order to prevent its agglomeration and welding. The crystallite size of the tested nanocrystalline aluminum samples was measured from XRD data using Scherrer equation and recorded only 28 nm.

2.2. Electrochemical cell

An electrochemical cell with a three-electrode configuration was used; a platinum foil and an Ag/AgCl electrode (in the saturated KCl) were used as the counter and reference electrodes, respectively. The traditional and nanocrystalline pure Al rods were used as the working electrode. Before immersing the different Al rods in the Arabian Gulf seawater, their examined surfaces were first grinded successively with metallographic emery paper of increasing fineness up to 800 grit and further polished with 5, 1, 0.5, and 0.3 mm alumina slurries (Buehler). The electrodes were then cleaned using doubly-distilled water, degreased with acetone, washed using doubly-distilled water again and finally dried with dry air.

2.3. Electrochemical test measurements

For all electrochemical experiments, an Autolab Potentiostat (PGSTAT20 computer controlled) operated by the general purpose electrochemical software (GPES) version 4.9 was used to perform the electrochemical experiments. The cyclic potentiodynamic polarization (CPP) curves were obtained by scanning the potential in the forward direction from -1600 to -250 mV against Ag/AgCl at a scan rate of 1.0mV/s. For the back scan, the potential was reversed in the backward direction at the same scan rate in order to complete the cycle test. Potentiostatic current-time experiments were carried out by stepping the potential of the aluminum samples at − 550 mV vs. Ag/AgCl for 40 min. The electrochemical impedance spectroscopy (EIS) tests were performed at corrosion potentials (E_{OCP}) over a frequency range of 100 kHz – 100 mHz, with an ac wave of ± 5 mV peak-to-peak overlaid on a dc bias potential, and the impedance data were collected using Powersine software at a rate of 10 points per decade change in frequency. All measurements were carried out at room temperature and after 1 hour immersion of the working electrode in the Arabian Gulf seawater except the open-circuit potential curves were collected from the first moment of the electrode immersion.

3. RESULTS AND DISCUSSION

3.1. Cyclic potentiodynamic polarization (CPP) measurements

Cyclic potentiodynamic polarization (CPP) has been the most used techniques in obtaining the parameters of corrosion and its control for metals and alloys in contact with aggressive media. The

CPP curves obtained for (a) microcrystalline and (b) nanocrystalline Al electrodes after their immersion for 40 minutes the Arabian Gulf seawater are shown respectively in Fig. 1. The values of corrosion potential (E_{Corr}), corrosion current (j_{Corr}), cathodic Tafel slope (β_c), anodic Tafel slope (βa), polarization resistance (R_P), and corrosion rate (R_{Corr}) obtained from the polarization curves shown in Fig. 1 are listed in Table 1. The values of the E_{Corr} and j_{Corr} were obtained from the extrapolation of anodic and cathodic Tafel lines located next to the linearized current regions. The values of R_{Corr} and R_P were calculated as has been reported in our previous studies [23-27]. It is clearly seen from Fig. 1a that the current decreases with potential in the cathodic branch until it reaches to the corrosion current density, where the cathodic reaction for aluminum in aerated near neutral solutions is primarily the reduction of oxygen followed by its adsorption through these two reactions [9,11];

$$\frac{1}{2}O_2 + H_2O_{(S)} + e^- = OH_{ads.} + OH^- \tag{1}$$

$$OH_{ads.} + e^- = OH^- \tag{2}$$
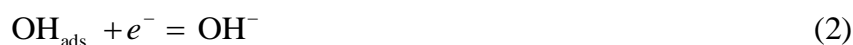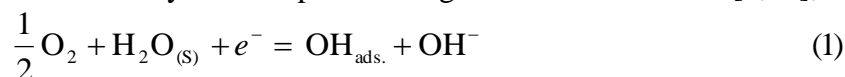
On the other hand, the current increases again in the anodic side because the reaction at this condition is the dissolution of metallic aluminum (Al^0) into aluminum cations (Al^{3+}) according to the following equation [9,11];

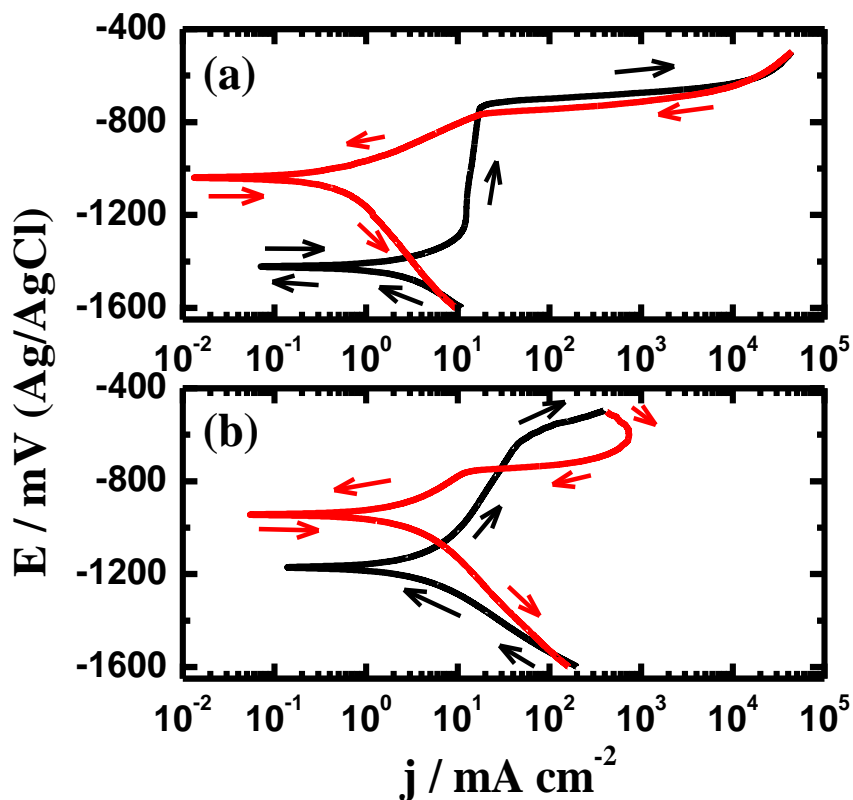$$Al = Al^{3+} + 3e^- \tag{3}$$

Figure 1. Cyclic potentiodynamic polarization curves obtained for (a) microcrystalline and (b) nanocrystalline Al electrodes after their immersion for 40 minutes the Arabian Gulf seawater.

The current then stays almost unchanged with large increase in the applied potential in the passive region seen on the curve. It has been reported [18] that aluminum hydroxide, $Al(OH)_3$, may form in the early stages of the anodic reaction before the transformation of this hydroxide into aluminum oxide, $Al_2O_3 \cdot 3H_2O$, as per the following reactions,

$$Al_{(S)} + 3OH^- = Al(OH)_{3,ads.} + 3e^- \qquad (4)$$

$$2Al(OH)_3, \text{ }_{ads.} = Al_2O_3.3H_2O \qquad (5)$$
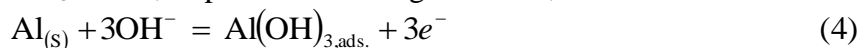
The formation of $Al_2O_3 \cdot 3H_2O$ largely protects the aluminum surface and leads to the long passive region seen on the CPP curve shown by Fig. 1a. This oxide film does not last on the aluminum surface and its breakdown takes place with increasing the potential in the less negative direction leading to the occurrence of pitting corrosion. The severity of pitting corrosion of aluminum also increased due to the presence of aggressive species such as chloride ions in the seawater medium [7,9]. The abrupt increase in the current values seen on the curve (Fig. 1a) can be explained by Eq. (1) as well as the reaction of Al with the chloride ions presented in the solution [9,11];

$$Al^{3+} + 4Cl^- = AlCl_4^- \qquad (6)$$

The aluminum chloride complex, $AlCl_4^-$, was formed on the surface and its presence increased the occurrence of pitting corrosion. This was indicated by the appearance of a large narrow hysteresis loop, which was formed due to the higher current values in the backward direction than the recorded currents in the forward one.

The CPP curve for the nanocrystalline aluminum, Fig. 1b, showed shorter passive region and bigger hysteresis loop as compared to that recorded for the microcrystalline aluminum. The shorter passive region was due to the dissolution of the aluminum surface as a result of the presence of more active centers in the nanocrystalline structure of the aluminum. The wider hysteresis loop confirms the more severity is the pitting corrosion for the nanocrystalline aluminum compared to the microcrystalline aluminum. This indicates that the surface of the nanocrystalline aluminum is more active, which allows it to be more susceptible to sever corrosion in the Arabian Gulf seawater. This was further indicated by the parameters listed in Table 1, where the nanocrystalline aluminum recorded higher j_{Corr} and R_{Corr} values as well as lower R_P value compared to the microcrystalline aluminum.

Table 1. Parameters obtained from polarization curves shown in Fig. 1 for Al electrodes immersed in the Arabian Gulf seawater for 40 min before measurements.

Electrode	Polarization parameters					
	β_c / $mVdec^{-1}$	E_{Corr} / mV	j_{Corr} / μAcm^{-2}	β_a / $mV\ dec^{-1}$	R_p / $k\Omega cm^2$	R_{Corr} / mmy^{-1}
Microcrystalline Al	175	-1425	3.85	180	10.02	0.042
Nanocrystalline Al	145	-1255	9.7	220	3.92	0.106

3.2. Potentiostatic current-time and scanning electron microscope (SEM) investigations

The current-time curves obtained for (1) microcrystalline Al and (2) nanocrystalline Al electrodes after their immersion in Arabian Gulf seawater for 40 minutes followed by stepping the potential to -0.550 V vs. Ag/AgCl are shown respectively in Fig. 2. It is obvious from Fig. 2 (curve 1) that the recorded current for the microcrystalline Al electrode rapidly increased in the first 400 s before slightly increased with increasing the time of the experiment. On the other hand, the nanocrystalline Al electrode (curve 2) showed similar behavior but with very high current values compared to the microcrystalline Al across the whole time of the experiment. The rapid increases of the current values for both micro and nanocrystalline Al electrodes was due to the dissolution of an aluminum oxide that was formed on the surface while it was immersed in the Arabian Gulf seawater for 40 min before applying the active potential, -550 mV vs. Ag/AgCl. The slight increase of current with time resulted from the occurrence of pitting corrosion as has been previously reported [9,11]. The current-time measurements thus indicate that the corrosion resistance of the Al surface was higher for the microcrystalline structure, while the dissolution of the nanocrystalline Al in the Arabian Gulf seawater was higher, which agrees with the polarization data.
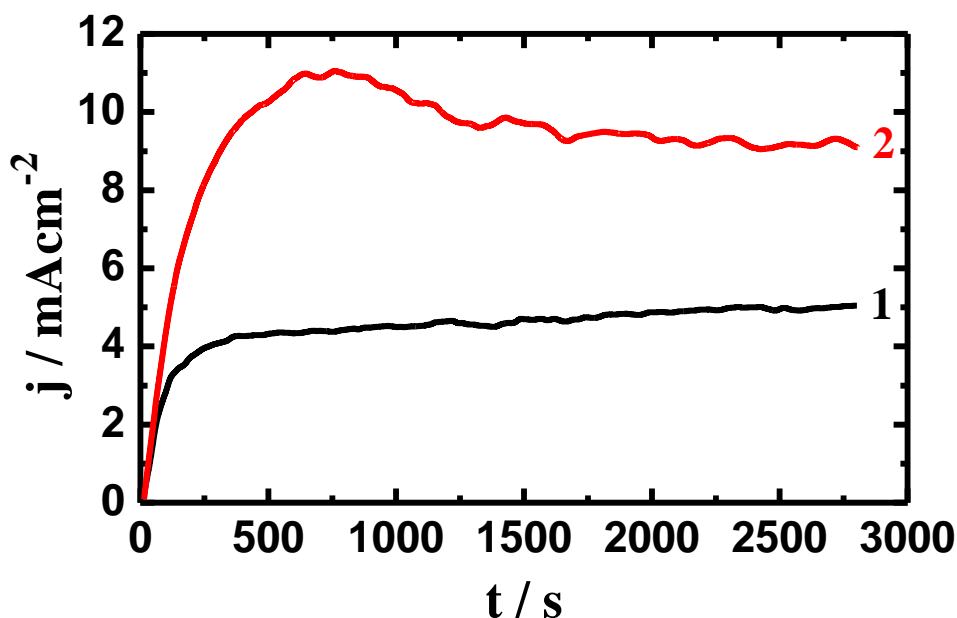

Figure 2. Chronoamperometric curves obtained for (1) microcrystalline Al and (2) nanocrystalline Al electrodes after their immersion in Arabian Gulf seawater for 40 minutes followed by stepping the potential to -0.550 V vs. Ag/AgCl.

In order to shed more light on the corrosion of the microcrystalline and nanocrystalline Al surfaces after their immersion in the Arabian Gulf seawater and applying high anodic potential, the SEM investigations were carried out. Fig. 3 depicts the SEM images for (a) microcrystalline Al and (b) nanocrystalline Al electrodes after their immersion in Arabian Gulf seawater for 40 minutes followed by stepping the potential to -550 mV vs. Ag/AgCl. It is clearly seen from the SEM images that the

nanocrystalline surface was more deteriorated and suffered higher corrosion compared to the nanocrystalline Al electrode. This means that the corrosion resistance of the nanocrystalline Al was low, which is due to the large surface area and the presence of many active centers. These properties for the nanocrystalline Al structure make it more susceptible for active dissolution under the applied potential and the aggressiveness attack for the Arabian Gulf seawater.
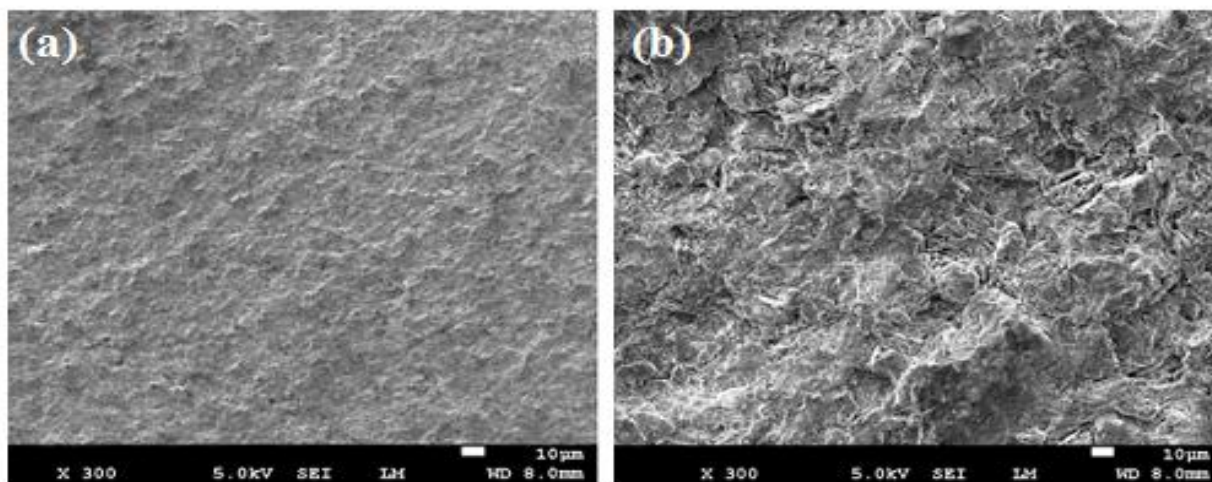

Figure 3. SEM images for (a) microcrystalline Al and (b) nanocrystalline Al electrodes after their immersion in Arabian Gulf seawater for 40 minutes followed by stepping the potential to -550 mV vs. Ag/AgCl.

3.3. Open-circuit potential (OCP) measurements

Fig. 4 shows the change of the OCP vs. time curves obtained for (1) microcrystalline Al and (2) nanocrystalline Al electrodes in Arabian Gulf seawater. On the first moment of Al immersion, the potential shifted towards the less negative direction for both micro and nanocrystalline electrodes. The recorded potential for the microcrystalline Al (curve 1) abruptly shifted to the lesser negative value (~ -925 mV vs. Ag/AgCl) in the first several seconds due to an aluminum oxide film thickening. The potential then slightly increased towards the more negative direction and finally stayed almost steady. This is due to the equilibrium between the oxide film thickening and its dissolution under the corrosiveness action for the Arabian Gulf seawater on the surface of Al.

On the other hand and after the initial less negative shift obtained for the nanocrystalline Al electrode, its potential increased towards the more negative values. Where, the potential of the nanocrystalline Al showed more negative values in the absolute potential (> 100 mV vs. Ag/AgCl) across the whole time of the experiment compared to the potential of microcrystalline Al. This is due to the dissolution of the aluminum oxide film that was initially formed on the surface of the nanocrystalline Al by the harsh attack of the Arabian Gulf seawater. The OCP vs. time behavior reveals that the nanocrystalline Al suffered more corrosion as a result of its larger surface area and the presence of more active centers compared to the microcrystalline Al electrode at the same condition.
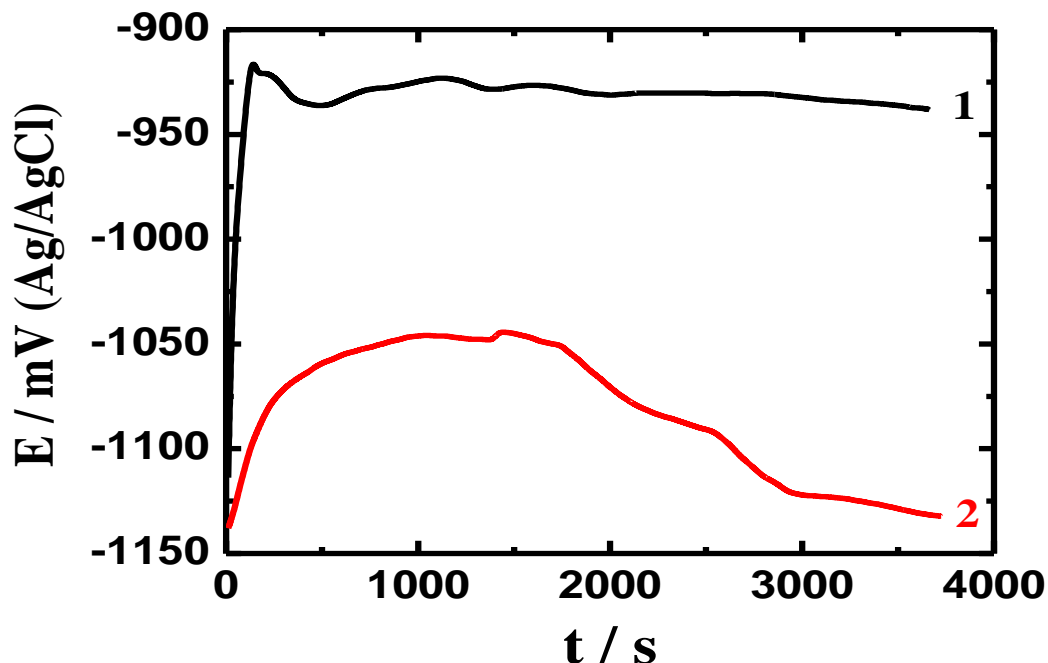
Figure 4. Open-circuit potential versus time curves obtained for (1) microcrystalline Al and (2) nanocrystalline Al electrodes in Arabian Gulf seawater.

3.4. Electrochemical impedance spectroscopy (EIS) investigations

The Nyquist plots obtained for (1) microcrystalline Al and (2) nanocrystalline Al electrodes after their immersion in Arabian Gulf seawater for 40 min are shown respectively in Fig. 5. These experiments were carried out in order to determine the mechanistic and kinetic parameters for the electrodes under investigation and to report the difference between their corrosion behaviors in the Arabian Gulf seawater. The spectra shown in Fig. 5 were analyzed by best fit to an equivalent circuit model that is shown in Fig. 6. The symbols represented in the equivalent circuit model can be defined as follows: R_S represents the solution resistance, Q_1 the constant phase elements (CPEs), R_{P1} the polarization resistance and can be defined as the charge transfer resistance of the cathodic reduction reaction of aluminum, Q_2 another constant phase elements and R_{P2} another polarization resistance [28]. The values of all these parameters are listed in Table 2. It is clearly seen from Fig. 5 that both Al electrodes showed a single semicircle whose diameter is wider for the microcrystalline Al rod. The semicircles at high frequency are generally associated with the relaxation of the capacitors of electrical double layers with their diameters representing the charge transfer resistances [28].

It is clearly seen from Table 2 that the values of R_S, R_{P1} and R_{P2} for the microcrystalline Al electrode are higher than those listed for the nanocrystalline electrode. This indicates that the corrosion resistance for the microcrystalline Al is higher and the dissolution is lower than its rate for the nanocrystalline electrode in the Arabian Gulf seawater. This was also confirmed by the low values of Q_1 and Q_2 for the microcrystalline Al. Here and according to the previous work [18], the CPE for the micro and nanocrystalline Al electrodes in the seawater can be defined as follows;

$$Z(CPE) = \left(\frac{Y_0 - 1}{(j\omega)^n} \right) \qquad (7)$$

Where, Y0 is the CPE constant, ω is the angular frequency (in rad s^{-1}), $j^2 = -1$ is the imaginary number and n is the CPE exponent. At this conditions, Q_1 and Q_2 with their n-values close to unity represent double layer capacitors with some porous in the structure of the film formed on the Al surface for both electrodes [9,11]. The EIS results thus confirm the data obtained by the dynamic polarization and potentiostatic polarization as well as the open-circuit potential measurements that the microcrystalline Al has higher resistance against the corrosion in the Arabian Gulf seawater at room temperature.
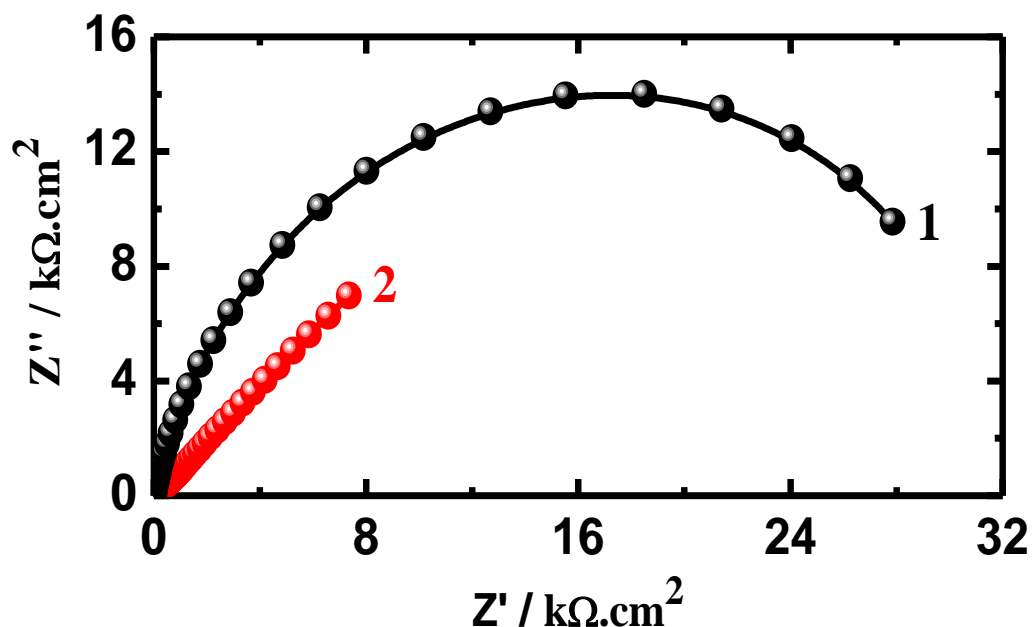

Figure 5. Typical Nyquist plots obtained for (1) microcrystalline Al and (2) nanocrystalline Al electrodes after their immersion in Arabian Gulf seawater for 40 minutes.
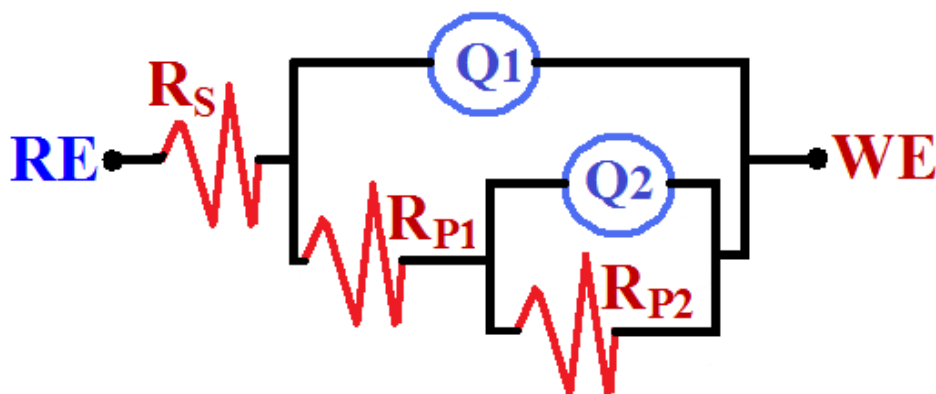

Figure 6. The equivalent circuit model used to fit the EIS experimental data depicted in Fig. 5; the symbols of the circuit are defined in text and their values are listed in Table 2.

Table 2. Parameters obtained by fitting the Nyquist plots shown in Fig. 5 with the equivalent circuit shown in Fig. 6 for microcrystalline and nanocrystalline Al electrodes after 40 min immersion in the Arabian Gulf sea water.

Electrode	Parameters						
	R_S / Ωcm^2	Q_1		R_{P1} / $k\Omega cm^2$	Q_2		R_{P2} / $k\Omega cm^2$
		Y_{Q1}/ μFcm^{-2}	n		Y_{Q2}/ μFcm^{-2}	n	
Microcrystalline Al	10.34	2.45	0.92	12.62	1.07	0.86	9.53
Nanocrystalline Al	7.27	5.81	0.84	6.78	2.52	0.80	3.36

4. CONCLUSIONS

The fabrication of a new nanocrystalline structure pure aluminum using mechanical alloying technique was reported. The corrosion of the nanocrystalline aluminum was studied and compared to a microcrystalline structure aluminum in a natural seawater was obtained from the Arabian Gulf. The corrosion behavior of these materials was performed using the cycling potentiodynamic polarization (CPP), potentiostatic current-time at constant potential (-550 mV vs. Ag/AgCl), open-circuit potential (OCP), and electrochemical impedance spectroscopy (EIS) measurements. The corrosion results indicated that the nanocrystalline aluminum showed higher anodic, cathodic and corrosion currents and corrosion rate than the ones obtained for the microcrystalline aluminum. This made the later more resistant to corrosion in the seawater compared to the nanocrystalline structure, which showed less polarization resistance. Results also revealed that the nanocrystalline aluminum showed sever uniform and pitting corrosion than the microcrystalline aluminum due to the small grain size and the high surface area that make it more susceptible to corrosion.

References

1. F.H. Latief, El-Sayed M. Sherif, A.A. Almajid, H. Junaedi, *J. Anal. Appl. Pyrolysis,* 92 (2011) 485.
2. G.M. Pinto, J. Nayak, A.N. Shetty, *Int. J. Electrochem. Sci.*, 4 (2009) 1452.
3. T. Choh, T. Oki, *Mater. Sci. Technol.,* 3 (1987) 378.
4. X. Lei, J. Ma, Y. Sun, *Int. J. Electrochem. Sci.,* 6 (2011) 537.
5. El-Sayed M. Sherif, Mahmoud S. Soliman, E.A. El-Danaf, A.A. Almajid, *Int. J. Electrochem. Sci.,* 8 (2013) 1103.
6. El-Sayed M. Sherif, A.A. Almajid, F.H. Latif, H. Junaedi, *Int. J. Electrochem. Sci.,* 6 (2011) 1085.
7. El-Sayed M. Sherif, E.A. El-Danaf, M.S. Soliman, A.A. Almajid, *Int. J. Electrochem. Sci.,* 7 (2012) 2846.

8. K.F. Khaled, *Corros. Sci.,* 52 (2010) 2905.
9. E.M. Sherif, S.-M. Park, *J. Electrochem. Soc.,* 152 (2005) B205.
10. Serpil Şafak, Berrin Duran, Aysel Yurt, Gülşen Türkoğlu, *Corros. Sci.,* 54 (2012) 251.
11. E.M. Sherif, S.-M. Park, *Electrochim. Acta*, 51 (2006) 1313.
12. G.Y. Elewady, I.A. El-Said, A.S. Fouda, *Int. J. Electrochem. Sci.,* 3 (2008) 177.
13. M. Nakamura, N. Ikemiya, A. Iwasaki, Y. Suzuki, M. Ito, *J. Eletroanal. Chem.* 566 (2004) 385.
14. A. Gebert, U. Wolff, A. John, J. Eckert, L. Schultz, *Mater. Sci. Eng*. A 299 (2001) 125.
15. R.V.S. Rao, U. Wolff, S. Baunack, J. Eckert, A. Gebert, *J. Mater. Res.* 18 (2003) 97.
16. X.Y. Wang, D. Y. Li, *Electrochim. Acta* 47 (2002) 3939.
17. Z. Liu, T. Wu, K. Dahm, F. Wang, *Scrip. Mater.,* 37 (2002) 1151.
18. El-Sayed M. Sherif, Hany Rizk Ammar, Khalil A Khalil, *Appl. Surf. Sci.*, 301 (2014) 142–148.
19. Li Liu, Ying Li, Fuhui Wang, *J. Mater. Sci. Technol.* 26 (2010) 1-14.
20. P. Queipo, M. Granda, R. Santamarîa, R. Menéndez, *Fuel*, 83 (2004) 1625.
21. P.K. Rohatgi, R. Asthana, S. Das, *Int. Met. Rev.*, 31 (1986) 115.
22. F. Akhlaghi, S.A. Pelaseyyed, *Mater. Sci. Eng*. A., 385 (2004) 258.
23. El-Sayed M. Sherif, Abdulhakim A. Almajid, *J. Chem.,* 2014 (2014) 1.
24. El-Sayed M. Sherif, *Appl. Surf. Sci.,* 292 (2014) 190.
25. El-Sayed M. Sherif, *Ind. Eng. Chem. Res.,* 52 (2013) 14507.
26. El-Sayed M. Sherif, A.H. Ahmed, *Synthesis and Reactivity in Inorganic, Metal-Organic, and Nano-Metal Chemistry*, 40 (2010) 365.
27. El-Sayed M. Sherif, Asiful H. Seikh, *J. Chem.,* 2013 (2013) Article ID 497823, 7 pages.
28. H. Ma, S. Chen, L. Niu, S. Zhao, S. Li, D. Li, *J. Appl. Electrochem.,* 32 (2002) 65.